14th International Conference on Applications of Statistics and Probability in Civil Engineering, ICASP14
Dublin, Ireland, July 9-13, 2023

Random Field Modeling of the Mechanical Properties of Graphene Nano-platelets

Panagiotis Gavallas
PhD Student, Dept. of Civil Engineering, Aristotle University of Thessaloniki, Thessaloniki, Greece

Dimitrios Savvas
Researcher, Dept. of Civil Engineering, Aristotle University of Thessaloniki, Thessaloniki, Greece

George Stefanou
Assoc. Professor, Dept. of Civil Engineering, Aristotle University of Thessaloniki, Thessaloniki, Greece

ABSTRACT: In this work, a random field approach is employed to model the mechanical properties of graphene nano-platelets (GNPs) consisting of multiple graphene sheets connected with van der Waals forces. GNPs share the excellent properties of single layer graphene and can be used as reinforcements in composite materials, yet these properties are affected by the presence of random structural defects. A parametric study is conducted herein, investigating the effect of defect type and density, as well as of the number of graphene layers on the mechanical properties of GNPs, which are simulated through the Molecular Structural Mechanics (MSM) approach with equivalent space frame FE models. The defect induced random spatial variation of the mechanical properties is accounted for using random fields, which are computed by employing the moving window technique and computational homogenization. Useful conclusions are derived and the resulting random property fields can be used in the stochastic finite element analysis of GNP-reinforced composites.

1. INTRODUCTION

Single layer graphene is essentially a 2-D material (1 atom thick) and exhibits excellent mechanical, thermal and electrical properties. With regard to its mechanical properties, measurements by Lee et al. (2008) show a Young's modulus of 1 TPa and a tensile strength of 130 GPa, making it the strongest material ever discovered. Its strength is attributed to its two-dimensional hexagonal carbon atom structure and extremely strong covalent C-C bonds. When embedded in a polymer matrix, even in small amounts, Song et al. (2018) show that it can greatly enhance the composite stiffness and is therefore considered an ideal reinforcement material. With regard to civil engineering applications, the addition of as little as 0.033% of graphene in the concrete mix can substantially increase tensile and compressive strength, as shown in e Silva et al. (2017).

However, techniques for efficient mass production of graphene are still to be found, limiting its current applications. Graphene nanoplatelets (GNPs), which consist of few layer graphene (up to 10 layers), offer similar properties for a smaller production cost, for example, by skipping the centrifugation steps in the liquid phase exfoliation production method, as mentioned by Cataldi et al. (2018). Considering an interlayer distance of 0.335 nm, the thickness of GNPs is in the order of a few nm, while their lateral size can be in the order of a few μm.

Similarly to single layer graphene, carbon atoms are arranged in a hexagonal lattice in the inplane direction, while the multiple graphene layers are held together mainly through van der Waals (vdW) forces.

In literature, one can find several studies on the mechanical properties of multilayer graphene. Molecular dynamics as well as FE methods are commonly employed to compute the equivalent Young's modulus, yielding various results, as shown by Chandra et al. (2020). However, as suggested by Hosseini Kordkheili and Moshrefzadeh-Sani (2013), when adjusted to the considered thickness, most works lead to an estimate of 1 TPa for the inplane Young's modulus. Additionally, this value does not appear to depend on the number of layers and graphene is shown to exhibit isotropic behavior for the case of small strains, as shown in Shokrieh and Rafiee (2010).

Structural defects, either preexisting or introduced during the production process, are certain to have a negative influence on the properties of GNPs, as Savvas and Stefanou (2018) show for the case of single layer graphene. Random vacancy defects lead to up to a 60% decrease in mean graphene stiffness, while random waviness is shown by Papadopoulos et al. (2017) to considerably reduce the stiffness of graphene reinforced composites. As shown by Kumar et al. (2021), defects located at the edge of the graphene sheet lead to a greater reduction of mechanical properties, while these properties are shown to be temperature dependent through Molecular Dynamics.

For the case of GNPs, however, limited research data is available on the effect of random structural defects on their mechanical behavior. Therefore, this work provides a detailed investigation on the influence of planar structural defects on the mechanical properties of GNPs.

2. Molecular structural mechanics approach

In this work, the Molecular Structural Mechanics (MSM) method is employed to simulate the graphene lattice. MSM is a continuum-based nanoscale modeling technique and was developed by Li and Chou (2003b). In this approach, the potential energy produced by C-C interactions is equated to the sum of energies produced by the deformations of a structural element (beam or truss), thus obtaining equivalent element properties. As a result, the graphene lattice is simulated with a space frame finite element model, which can be analyzed with standard FEM. Figure 1 shows an example of a GNP model with only a few vdW connecting elements shown for visualization purposes.

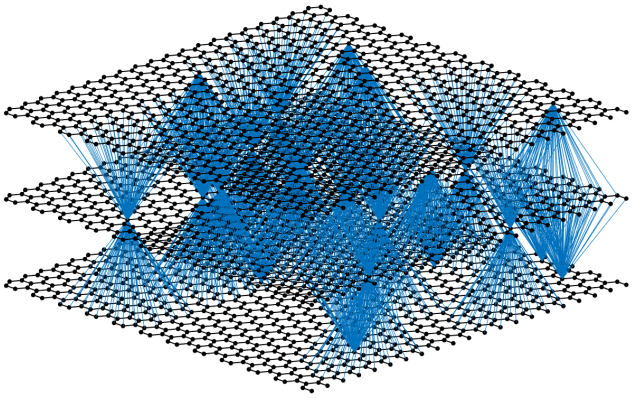

Figure 1: Finite element model of a three layer GNP with limited vdW elements visible.

2.1. C-C covalent bonds

The mechanical behavior of graphene is determined by the carbon atom interactions, which are governed by a molecular force field. The total potential energy of this force field can be described with the following equation:

$$U = U_r + U_\theta + U_\phi + U_\omega + U_{vdW} + U_{es} \qquad (1)$$

where $U_r, U_\theta, U_\phi, U_\omega$ are the bond-stretching energy, the bond-angle variation energy, the dihedral-angle torsion energy and the inversion (out of plane torsion) energy, respectively. U_{vdW} and U_{es} are associated with non-bonded van der Waals and electrostatic interactions, respectively, which are usually negligible and are therefore omitted.

Following the MSM approach, the covalent C-C bonds are modeled with circular beam finite elements and by equating the deformation energy potential of the beam element to the potential of the

molecular force field, the following circular beam properties are obtained (see Savvas and Stefanou (2018)): diameter d = 0.147 *nm*, Young's modulus E = 5.49 TPa and shear modulus G = 0.871 TPa.

2.2. *Van der Waals forces*

The multiple layers in GNPs are connected with van der Waals forces, which are often modeled using the Lennard-Jones potential according to Jones and Chapman (1924). As a result, these forces are given as a function of the distance of interacting atoms through the following equation:

$$F(r) = 24\varepsilon/\sigma[2(\sigma/r)^{13} - (\sigma/r)^{7}] \qquad (2)$$

where $\varepsilon = 0.0556\ kcal/mol$, $\sigma = 0.335\ nm$ and r is the interatomic distance. Figure 2 shows the relation between the vdW force magnitude and the distance between two carbon atoms.

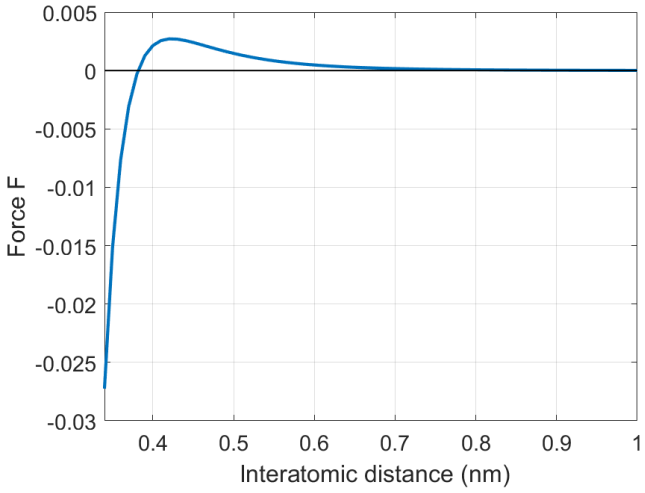

Figure 2: vdW force as a function of interatomic distance.

Linear truss elements are employed to model the vdW interactions. These elements have the same length as the connected interlayer carbon atoms and their stiffness varies depending on their length, in order to satisfy Eq. (2). Since vdW forces become negligible at distances greater than 2.5σ ($0.84nm$), no connecting truss elements are added between carbon atoms whose distance is greater than 2.5σ. For simplification purposes, it is further assumed there are no vdW interactions between carbon atoms of non-neighboring layers. Note that vdW forces are considerably weaker than the in-plane covalent bonds, thus it can be considered that graphene sheets are loosely connected in the out of plane direction.

2.3. *Structural defects*

The properties of graphene can be substantially affected by the presence of defects in its lattice structure. Figure 3 shows the three types of structural defects examined in this work: Stone Wales (SW), single vacancy (SV) and double vacancy (DV) defects. SW defects are crystallographic and occur after the connectivity of two bonded carbon atoms changes, resulting in their rotation by 90 degrees relative to the midpoint of their bond. These defects are also known as 5-7-7-5 defects, since the four adjacent hexagonal unit cells are transformed into two pentagonal and two heptagonal unit cells due to rotation. Vacancy defects occur when any number of carbon atoms, as well as their respective bonds, are removed from the graphene lattice. In the case of SV defects, only one carbon atom is missing while for DV defects, two adjacent carbon atoms are missing from the graphene lattice.

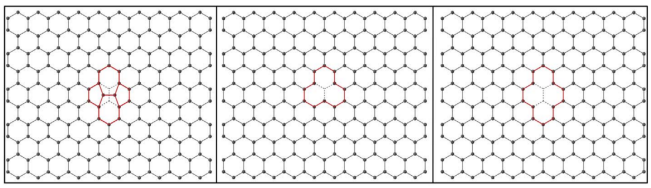

Figure 3: Types of defects in the graphene lattice, from left to right: SW, SV, and DV defects.

3. Computation of inplane properties

In this work the inplane mechanical properties of multilayer graphene are investigated, which are orders of magnitude higher than the out of plane properties, as shown by Hajgató et al. (2013). The equivalent stiffness of a GNP is computed from its microstructure using a homogenization like procedure by Miehe and Koch (2002), which can also be employed for cases of lack of material, such as in the presence of voids. The boundary nodes of the simulated GNP model are identified and suitable

boundary conditions are applied, in order to obtain the macroscopic stiffness tensor. The inplane stress-strain relation for an anisotropic material is given by the following equation:

$$\begin{bmatrix} \sigma_1 \\ \sigma_2 \\ \sigma_3 \end{bmatrix} = \begin{bmatrix} C_{11} & C_{12} & C_{13} \\ & C_{22} & C_{23} \\ symm. & & C_{33} \end{bmatrix} \begin{bmatrix} \varepsilon_1 \\ \varepsilon_2 \\ \varepsilon_3 \end{bmatrix} \quad (3)$$

Since the lattice of graphene contains random defects, its properties will also be random. The random field approach is employed herein, which is commonly used to model the random spatial variation of the properties of composite materials, as shown, e.g., in Stefanou et al. (2017). According to Baxter and Graham (2000), this is done by partitioning the structure domain into subdomains with the moving window technique and applying homogenization to each one of them. The resulting properties, considered at the midpoint of each window, can be used to reconstruct the random property field. While GNPs have a 3-D structure, 2-D random fields at the middle plane are computed in this work, considering their extremely small thickness (1 layer = 0.335 *nm*) compared to the lateral size, which can reach up to a few μm. Note that the equivalent properties are computed with the assumption that no delamination occurs and loading can be distributed uniformly, which is not always the case, as shown by Li and Chou (2003a) in carbon nanotubes (CNTs).

4. Results

In this section, the inplane mechanical properties of (50 $nm \times 50$ nm) GNPs are presented in random field form. The thickness h of GNPs depends on the number of layers n and is given by $h = n \times 0.335$ nm. The effect of different numbers of layers, defect types and densities is first examined for a window size of 5 nm. Initially, defects are distributed evenly across layers while an uneven defect distribution is subsequently taken into account. The effect of different moving window sizes is also investigated.

4.1. Effect of defect type and density

In this section the effect of both defect type and density is examined for different numbers of layers. Figure 4 shows the computed realizations of the random field of the elasticity component C_{11} along with the empirical distribution and autocorrelation function, for the case of triple layer graphene and 12% defect density for various types of defects. Results show a considerable drop in mean stiffness for the case of vacancy defects. The stiffness COV is also higher for vacancy defects, but the different defect types do not severely impact variability, with a maximum of 5.8% being recorded for DV defects.

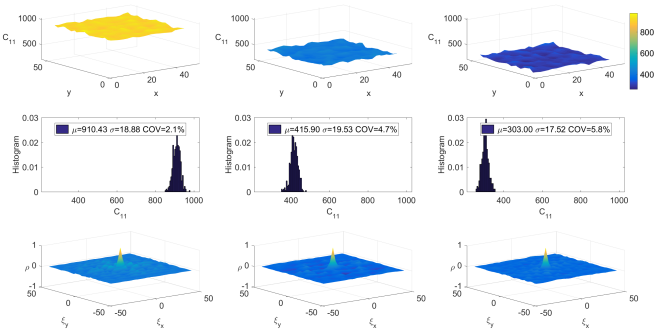

Figure 4: Random fields of stiffness component C_{11} for triple layer graphene and various defects at 12 % density. From left to right: SW, SV, DV defects.

Figures 5, 6 show the statistics of the random property fields of the stiffness component C_{11} for different numbers of layers and defect types. The stiffness component C_{22} exhibits nearly identical behavior to C_{11} and graphene can be regarded as approximately isotropic in the inplane direction. The properties of pristine graphene sheets, with inplane dimensions (5 $nm \times 5$ nm), are also shown for comparison purposes. Pristine axial stiffness exceeds 1 TPa, in accordance with literature findings. The results show nearly identical mean properties for any number of layers. A substantial decrease in the mean properties is observed in the case of vacancy defects, reaching a maximum of around 70% for DV defects and 12% density. The COV appears to decrease with the increasing number of layers, with a maximum of around 9.5% being recorded for single layer graphene at 12% DV defect density.

With regard to the inplane shear stiffness C_{33}, the effect of random defects is very similar to the one observed for the axial stiffness. Figure 7 shows the random fields of stiffness component C_{33} for 12%

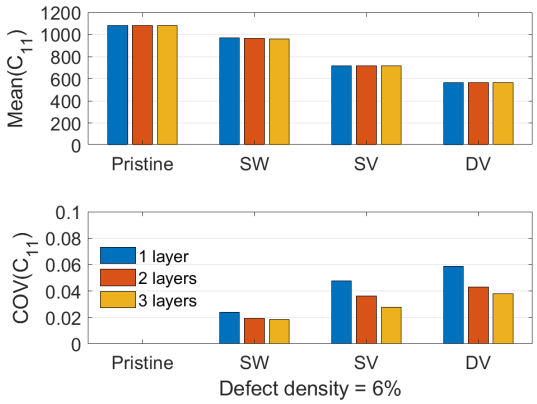

Figure 5: Mean and COV of random fields of stiffness component C_{11} for 6% defect density.

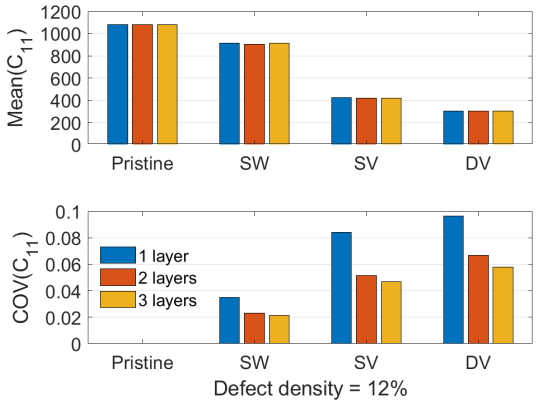

Figure 6: Mean and COV of random fields of stiffness component C_{11} for 12% defect density.

defect density while Figures 8, 9 show the mean and COV for several types of defects at 6 and 12% defect densities. Pristine inplane shear stiffness can reach up to a magnitude of 450 GPa. Similarly to the axial case, the mean properties are sharply reduced in the case of vacancy defects, while the maximum COV does not exceed 10%.

For all inplane stiffness components, the means do not appear to be particularly affected by the number of layers whereas the COV decreases with an increasing number of layers. The inplane behavior of GNPs in one direction can be regarded as equivalent to that exhibited by n springs connected in parallel. Note that the contribution of the vdW forces to the inplane properties is negligible.

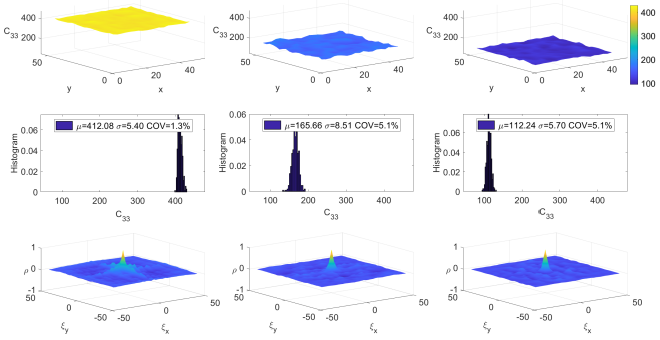

Figure 7: Random fields of stiffness component C_{33} (inplane shear) for triple layer graphene and various defect types at 12% density. From left to right: SW, SV, DV defects.

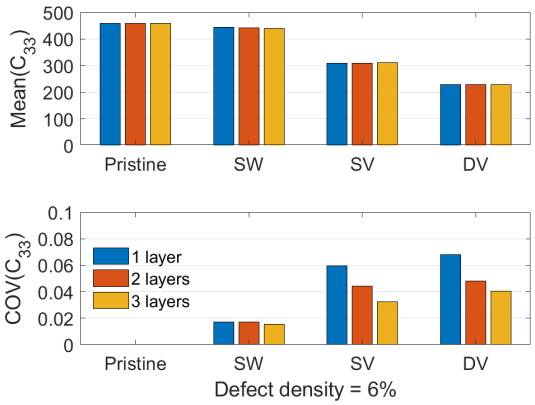

Figure 8: Mean and COV of random fields of stiffness component C_{33} (inplane shear) for 6% defect density.

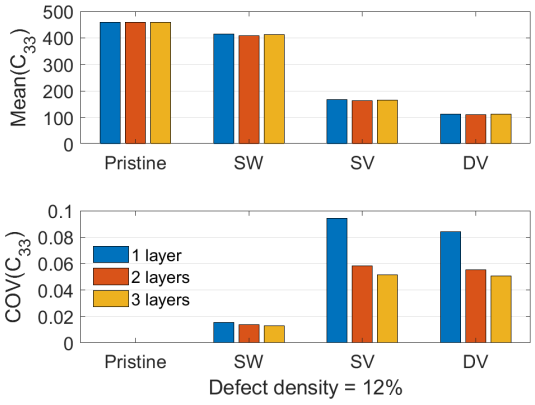

Figure 9: Mean and COV of random fields of stiffness component C_{33} (inplane shear) for 12% defect density.

4.1.1. Uneven defect distribution across layers

Until now, the same defect density was considered for all the layers of the GNP. In contrast to sin-

gle layer graphene, GNPs can have varying numbers of defects in each layer. In order to study the effect of uneven defect distributions across the constituent layers of GNPs, the defect density is kept constant over the entire GNP (e.g., 12%), but defects are moved towards a single layer and random fields of the mechanical properties are computed. For double layer graphene, defects are shifted towards one of the two layers, while in triple layer graphene, two different scenarios are considered, as defects can be either concentrated in the outer layer or in the middle layer.

For a particular defect density, the GNP contains m total defects. These are initially evenly distributed across layers, meaning each layer has $(1/n) \times m$ defects, where n is the number of layers. In this subsection, one particular layer is considered to contain $\alpha \times m$ defects, according to a ratio α. Three cases for this ratio are considered: $\alpha = 1/n$ (even distribution over the GNP), $\alpha = 2/3$ and $\alpha = 1$ (all defects concentrated in one layer). For a defect density of 12% over the entire GNP, the case $\alpha = 1$ would result in one layer having a density of 24% in double layer graphene or 36% in triple layer graphene, with the rest of the layers being defect-free.

Figures 10,11 show the mean and COV for 12% SV defects in double and triple layer graphene for the three cases mentioned above. The results refer to stiffness component C_{11} and show little difference for the other components. As defects are moved towards one layer, the mean properties are substantially increased, while the COV is decreased. This effect is more pronounced in triple layer graphene and can be explained by the lessening contribution of each layer to the total stiffness, as the number of layers increases. Hence, the layer which contains a large amount of defects will have a smaller impact on the overall stiffness. The pristine or less affected layers can compensate for the loss of stiffness of the layer containing the most defects, since the homogenized GNP stiffness is computed as an average over the considered volume and no delamination is observed. It is evident that an uneven defect distribution can lead to higher stiffness and less variability compared to having the same number of defects in each constituent GNP layer.

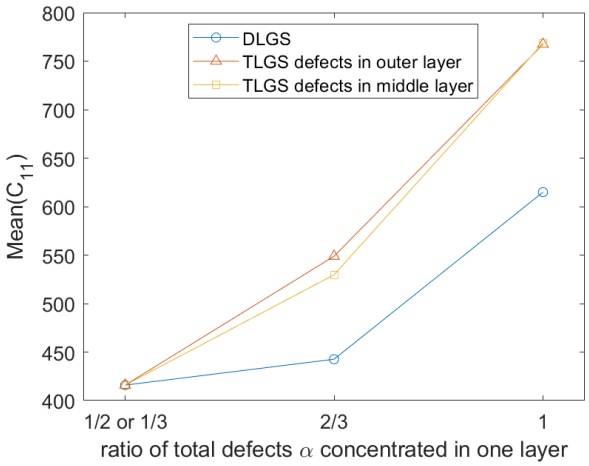

Figure 10: Mean plot of the random fields of stiffness component C_{11} for double (DLGS) and triple layer graphene sheets (TLGS) and an uneven defect distribution across layers, 12% SV defects. For an even defect distribution, $\alpha = 1/2$ for DLGS and $\alpha = 1/3$ for TLGS.

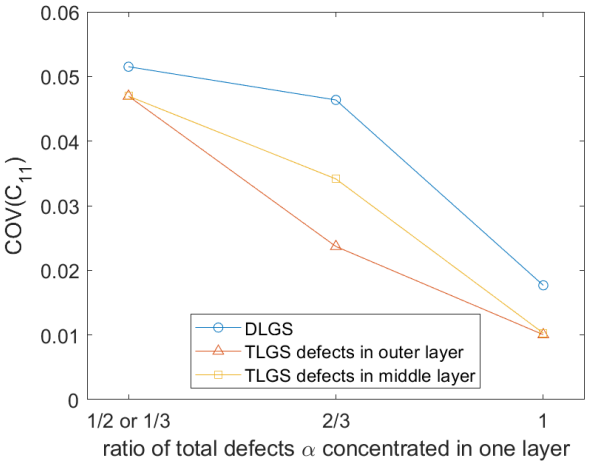

Figure 11: COV plot of the random fields of stiffness component C_{11} for double (DLGS) and triple layer graphene sheets (TLGS) and an uneven defect distribution across layers, 12% SV defects. For an even defect distribution, $\alpha = 1/2$ for DLGS and $\alpha = 1/3$ for TLGS.

4.2. Effect of moving window size

In this section, the effect of the moving window size is examined. The choice of window size can severely impact the spatial variability of the random field and extremely small or large sizes can lead to unrealistic results. The window sizes of 2.5 *nm* and

5 *nm* are compared herein, through which 1521 and 361 windows are obtained, respectively.

Figure 12 shows the computed random field, empirical distribution and autocorrelation function of stiffness component C_{11}, for the two different window sizes. The increased spatial variability for the smaller window size is obvious, leading to increased COV as well as decreased correlation lengths. Compared to all previously depicted results, which referred to the window size of 5*nm*, the increased spatial variability for a window size 2.5 *nm* is expected to also increase the stiffness COV.

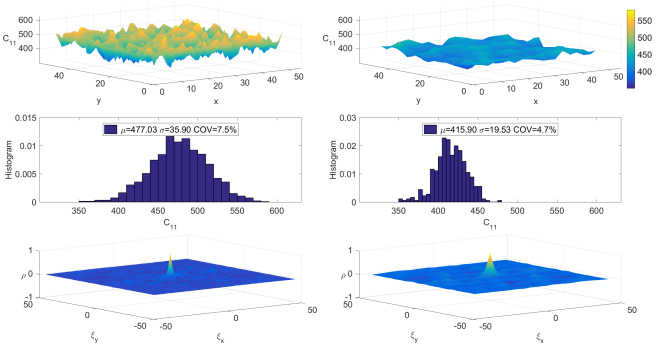

Figure 12: Random fields of stiffness component C_{11} in triple layer graphene for two different window sizes, 12% SV defects.

Figures 13, 14 show the mean and COV of the computed random fields for different types of defects and a defect density of 12%. As the moving window size is decreased, the mean is slightly increased, whereas a noticeable increase is observed in the COV for all numbers of layers. For both window sizes, the mean properties do not change with the number of layers, while the COV follows the previously observed decreasing trend with an increasing number of layers. The maximum COV is again observed for DV defects and single layer graphene, with its value being increased from 9.5% for the window size of 5 *nm* to 13% for the window size of 2.5 *nm*.

5. CONCLUSIONS

A parametric investigation was conducted on the effect of different numbers of layers, defect types and densities on the inplane mechanical properties

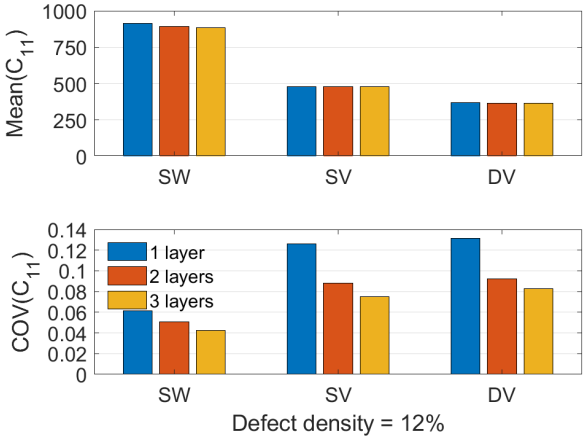

Figure 13: Mean and COV of random fields of stiffness component C_{11} for a moving window size of 2.5 *nm.*

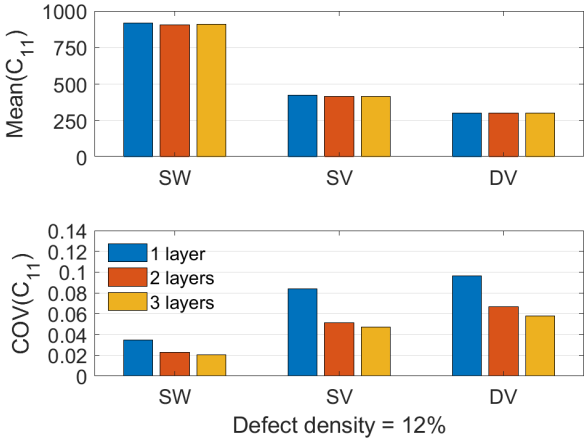

Figure 14: Mean and COV of random fields of stiffness component C_{11} for a moving window size of 5 *nm.*

of GNPs. Vacancy defects are shown to considerably decrease the mean stiffness, which often drops below 50% of its original value, while also demonstrating an increased COV. Results show constant mean properties regardless of the number of layers, while the COV appears to decrease with an increasing number of layers. These findings, along with the low stiffness of vdW elements connecting the individual layers, suggest that the inplane behavior of GNPs resembles a parallel spring model, where identical boundary conditions are applied to each spring and the resulting stiffness is finally averaged over the equivalent volume. In future works, a complete SFE analysis of a GNP-reinforced composite can be conducted, taking advantage of the computed random elasticity tensors.

ACKNOWLEDGEMENTS

The GREYDIENT project leading to this application has received funding from the European Union's Horizon 2020 research and innovation program under the Marie Skłodowska-Curie grant agreement No 955393.

REFERENCES

Baxter, S. and Graham, L. (2000). "Characterization of random composites using moving-window technique." *Journal of Engineering Mechanics*, 126(4), 389–397.

Cataldi, P., Athanassiou, A., and Bayer, I. S. (2018). "Graphene nanoplatelets-based advanced materials and recent progress in sustainable applications." *Applied Sciences*, 8(9), 1438.

Chandra, Y., Adhikari, S., Saavedra Flores, E., and Figiel, L. (2020). "Advances in finite element modelling of graphene and associated nanostructures." *Materials Science and Engineering: R: Reports*, 140, 100544.

e Silva, R. A., de Castro Guetti, P., da Luz, M. S., Rouxinol, F., and Gelamo, R. V. (2017). "Enhanced properties of cement mortars with multilayer graphene nanoparticles." *Construction and Building Materials*, 149, 378–385.

Hajgató, B., Güryel, S., Dauphin, Y., Blairon, J.-M., Miltner, H. E., Van Lier, G., De Proft, F., and Geerlings, P. (2013). "Out-of-plane shear and out-of plane young's modulus of double-layer graphene." *Chemical Physics Letters*, 564, 37–40.

Hosseini Kordkheili, S. and Moshrefzadeh-Sani, H. (2013). "Mechanical properties of double-layered graphene sheets." *Computational Materials Science*, 69, 335–343.

Jones, J. E. and Chapman, S. (1924). "On the determination of molecular fields.—i. from the variation of the viscosity of a gas with temperature." *Proceedings of the Royal Society of London. Series A, Containing Papers of a Mathematical and Physical Character*, 106(738), 441–462.

Kumar, Y., Sahoo, S., and Chakraborty, A. K. (2021). "Mechanical properties of graphene, defective graphene, multilayer graphene and sic-graphene composites: A molecular dynamics study." *Physica B: Condensed Matter*, 620, 413250.

Lee, C., Wei, X., Kysar, J. W., and Hone, J. (2008). "Measurement of the elastic properties and intrinsic strength of monolayer graphene." *Science*, 321(5887), 385–388.

Li, C. and Chou, T.-W. (2003a). "Elastic moduli of multi-walled carbon nanotubes and the effect of van der waals forces." *Composites Science and Technology*, 63(11), 1517–1524 Modeling and Characterization of Nanostructured Materials.

Li, C. and Chou, T.-W. (2003b). "A structural mechanics approach for the analysis of carbon nanotubes." *International Journal of Solids and Structures*, 40(10), 2487–2499.

Miehe, C. and Koch, A. (2002). "Computational micro-to-macro transitions of discretized microstructures undergoing small strains." *Archive of Applied Mechanics*, 72(4-5), 300–317.

Papadopoulos, V., Seventekidis, P., and Sotiropoulos, G. (2017). "Stochastic multiscale modeling of graphene reinforced composites." *Engineering Structures*, 145, 176–189.

Savvas, D. and Stefanou, G. (2018). "Determination of random material properties of graphene sheets with different types of defects." *Composites Part B: Engineering*, 143, 47–54.

Shokrieh, M. M. and Rafiee, R. (2010). "Prediction of young's modulus of graphene sheets and carbon nanotubes using nanoscale continuum mechanics approach." *Materials and Design*, 31(2), 790–795.

Song, M., Yang, J., and Kitipornchai, S. (2018). "Bending and buckling analyses of functionally graded polymer composite plates reinforced with graphene nanoplatelets." *Composites Part B: Engineering*, 134, 106–113.

Stefanou, G., Savvas, D., and Papadrakakis, M. (2017). "Stochastic finite element analysis of composite structures based on mesoscale random fields of material properties." *Computer Methods in Applied Mechanics and Engineering*, 326, 319–337.